Research on Chemical Intermediates (2020) 46:5417–5440
https://doi.org/10.1007/s11164-020-04270-0

New *β*-isatin aldehyde-*N,N′*-thiocarbohydrazones: preparation, spectroscopic studies and DFT approach to antioxidant characteristics

Hasan Yakan[1] · Temel Kan Bakır[2] · M. Serdar Çavuş[3] · Halit Muğlu[2]

Received: 23 June 2020 / Accepted: 5 September 2020 / Published online: 17 September 2020

Abstract

Five new Schiff bases of isatin and its derivatives were prepared from monothiocarbohydrazides and 5-chloro isatin. The chemical structures of the synthesized compounds were performed by ^{1}H NMR, ^{13}C NMR, and FT-IR spectroscopic techniques and elemental analysis. The in vitro antioxidant activities of all the products were determined by 1,1-Diphenyl-2-Picryl Hydrazyl free radical scavenging method. It also examined the antioxidant properties of the compounds based on quantum chemical calculations as well as supporting experimental spectroscopic data. Theoretical calculations carried out at B3LYP correlation functional with 6-311++g(2d,2p) basis set. Some chemical reactivity descriptors obtained from AIM, NCI, and ELF analysis were used to reveal the relationship between the electronic and antioxidant properties of the compounds. Furthermore, the bond lengths, charge densities, potential energy densities, inter-atomic dipole moments, and delocalization indices of the active phenolic hydrogen bonds of the compounds were shown to be parameters that can be used to determine the antioxidant properties of compounds.

Graphic Abstract

New *β*-isatin aldehyde-*N,N′*-thiocarbohydrazones were synthesized. Structures of synthesized molecules were clarified using spectroscopic methods. Antioxidant

Electronic supplementary material The online version of this article (https://doi.org/10.1007/s11164-020-04270-0) contains supplementary material, which is available to authorized users.

✉ Hasan Yakan
hasany@omu.edu.tr

✉ M. Serdar Çavuş
mserdarcavus@kastamonu.edu.tr

[1] Department of Mathematics and Science Education, Faculty of Education, Ondokuz Mayis University, Samsun, Turkey

[2] Department of Chemistry, Faculty of Art and Science, Kastamonu University, Kastamonu, Turkey

[3] Biomedical Engineering Department, Faculty of Engineering and Architecture, Kastamonu University, Kastamonu, Turkey

activities of the compounds were tested by the DPPH method. AIM, NCI, and ELF analysis were performed to investigate the relationship between the electronic properties and antioxidant activity.

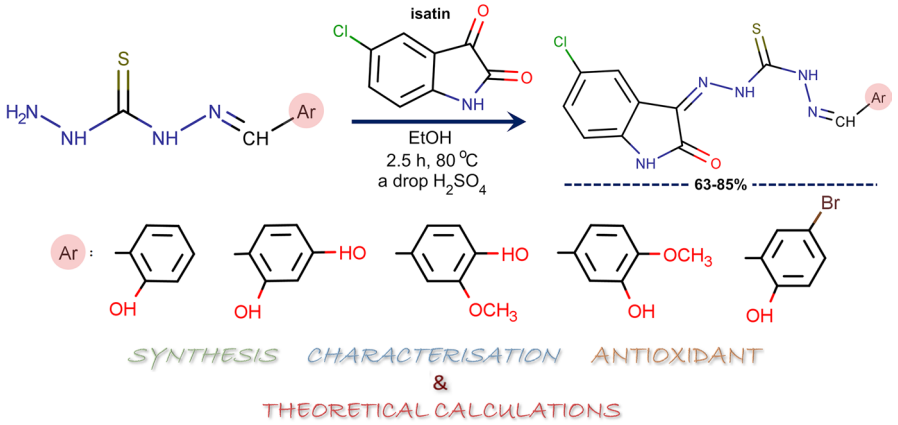

Keywords Schiff bases · Antioxidant assay · Spectroscopic techniques · AIM · NCI · ELF analysis

Introduction

Isatin and its derivatives are a significant class of hetero-compounds in organic chemistry. They have been reported to show several biological activities and applications in pharmaceutical chemistry [1–5]. They were reported as anti-bacterial [2], antiviral [3], antifungal [4], antioxidant [6, 7], anticonvulsant [8], anti-tubercular [9], and anti-HIV [10].

Schiff bases are compounds containing an azomethine group (–CH=N–) and can be easily synthesized via the condensation of primary amine with either an aldehyde or ketone. They are a significant class of compounds in the pharmaceutical and biological fields [11]. Isatin-based Schiff bases have a broad range of medicinal and pharmaceutical properties including anticonvulsant [8], antibacterial [12], anti-HIV, and antifungal activity [13]. Substituted isatin-thiocarbohydrazones based on Schiff bases are commonly called as β-isatin aldehyde-*N*,*N*′-thiocarbohydrazones. They display broad-spectrum pharmacological and biological properties such as antitumor [14–16], antimicrobial and antioxidant [17], cytotoxicity, anti-influenza virus, and antiviral activity [18].

Reactive oxygen species are produced by biochemical reactions and are controlled by antioxidant molecules in the body. Substances that delay or prevent oxidation of a substrate, such as inactivating singlet oxygen or providing H, are referred to as antioxidants [19]. Nowadays, many studies have been carried out to develop substances that exhibit more potent antioxidant activity. Kiran et al. [20] carried out the

synthesis of microwave-assisted β-isatin aldehyde-*N,N*-thiocarbohydrazone derivatives and reported that these molecules show antioxidant activities. Premanathan et al. [21] showed that isatin exhibits antioxidant activity in HL60 cells.

Understanding the mechanisms of antioxidant activity of the compounds requires a detailed determination and analysis of electronic and molecular properties [22–25]. One of the aims of this study is to provide a better understanding of the antioxidant activity mechanism by using DFT, non-covalent interaction (NCI), electron localization function (ELF), and atom in molecule (AIM) analyses. Moreover, the relationships between highest occupied molecular orbital (HOMO)–lowest unoccupied molecular orbital (LUMO) energies, electron affinity (EA), electronegativity (χ), ionization potential (IP), and chemical hardness (η) and antioxidant characteristics of the compounds were analyzed and the results used to explain the antioxidant activity.

Experimental section

Measurement and reagents

All reagents and solvents were purchased from Aldrich, Sigma, or Merck Chemical Company and were used without further purification. The solvents were spectroscopic grade. Melting points were recorded using Stuart melting point 30 apparatus and were uncorrected. The elemental analysis was measured on Eurovector EA3000-Single. Bruker Alpha FT-IR spectrometer was used for infrared spectra. ^{1}H and ^{13}C NMR spectra were taken on JEOL ECX-400 (400 MHz) in DMSO-d_6 spectrophotometer. Absorption measurements were recorded with SHIMADZU UV Pharmaspec 1700 spectrophotometer (Shimadzu Corp., Kyoto, Japan manufactures) with a pair of identical quartz cuvette of 1 cm thickness.

Synthesis of monothiocarbohydrazides (I–V)

Substituting aldehydes (2.50 mmol) and thiocarbohydrazide (3.00 mmol) in 20 mL of absolute ethanol, two drops of acetic acid were added into a (100 mL) bottom flask and reaction mixture refluxed 2.5 h at 80 °C. The solids formed were filtered off, washed with ethanol (75%), and dried to give the products. The reaction is shown in Scheme 1. Two of the synthesized compounds were new in the first step.

Synthesis of β-isatin aldehyde-*N,N′*-thiocarbohydrazones (VI–X)

An equimolar mixture of monothiocarbohydrazone and isatin in 20 mL of absolute ethanol, a drop of sulfuric acid was added to into a (100 mL) bottom flask and reaction mixture refluxed 2.5 h at 80 °C. The solids formed were filtered off, washed with ethanol (75%), and dried to give the products. The reaction is shown in Scheme 2. All the synthesized compounds were new in this step.

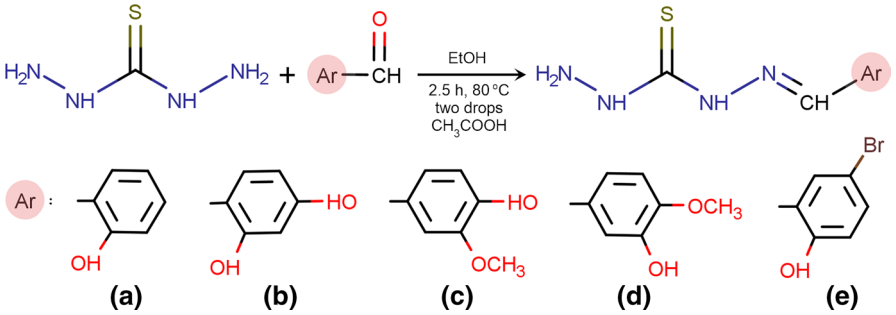

Scheme 1 General synthesis of monothiocarbohydrazones

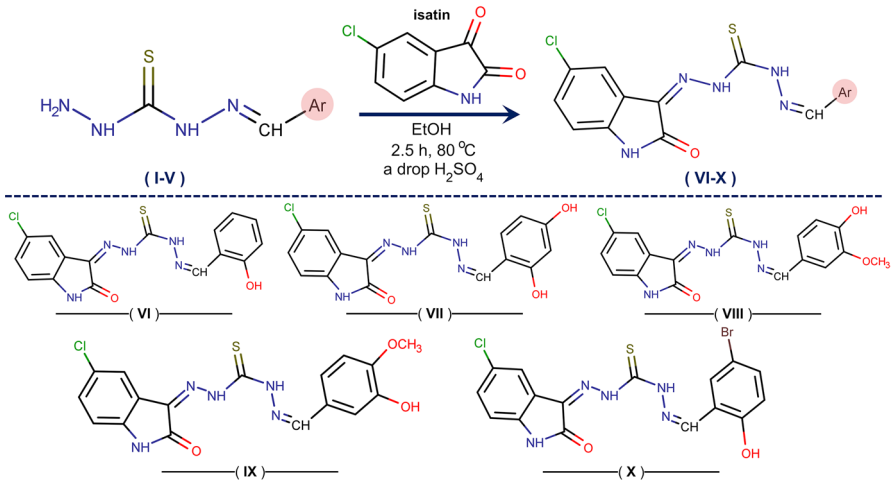

Scheme 2 General synthesis of *β*-isatin aldehyde-*N,N′*-thiocarbohydrazones

Antioxidant activity

For the determination of antioxidant activities of the compounds, a stock solution of 1,1-Diphenyl-2-Picryl Hydrazyl (DPPH) was first prepared at a concentration of 1.90×10^{-4} M. Then, solutions of compounds prepared in dimethyl sulfoxide (DMSO) (0.25 µM, 0.50 µM, 1.00 µM, 2.50 µM, and 5.00 µM) were determined. To this end, DPPH solutions prepared with ethanol were incubated in the dark for 30 min at room temperature and measurements were taken at 517 nm [26]. The percentage of radical damping activity was calculated by the following formula:

$$\%\text{inhibition} = \left[\left(A_0 - A_1\right)/A_0\right] \times 100$$

Here A_0 indicates the absorbance of the solution without synthesized compounds and A_1 the absorbance of the sample solution containing synthesized compounds [27]. The IC_{50} parameter commonly used to measure antioxidant activities of the

compounds was determined from the formula curve $y = mx + c$ obtained from the inhibition (%)-concentration plot [28].

Computational details

All the DFT [29, 30] calculations were performed with Gaussian 09 software [31] using the B3LYP exchange-correlation functional without any geometric constraints on the compounds. As a first step, the compounds were scanned dihedrally, as given in Fig. 1, to determine the minimum energy conformation of the compounds by using B3LYP/6-31g(d) level of theory, performing 360 steps with a rotation of 20°. No imaginary frequencies were observed in the calculations, i.e., optimized state geometries correspond to the actual minimum points on the potential surface. Conformational geometries with minimum energy obtained from the dihedral scanning were used as input data for all other calculations at the level of 6-311++g(2d,2p) basis set.

Optimizations of the compounds were performed in the gas phase, using B3LYP functional with 6-311++g(2d,2p) basis set. The frontier molecular orbital (FMO) energy eigenvalues were used to calculate global chemical reactivity parameters such as chemical hardness and electronegativity. The charge distribution on the individual atoms of the compounds was determined using the population analysis of natural bond orbitals (NBOs) [32–36]. Moreover, ^{1}H and ^{13}C NMR calculations were performed using optimized geometries. The NMR calculations were carried out using the Gauge-independent atomic orbital (GIAO) method in dimethyl sulfoxide (DMSO) phase in accordance with the experiments. Relative chemical shift values were calculated by subtracting the tetramethylsilane (TMS) shielding (31.8821 ppm for ^{1}H NMR, 182.4656 for ^{13}C NMR). The numbered form of the atoms of the compounds is given in Fig. 1.

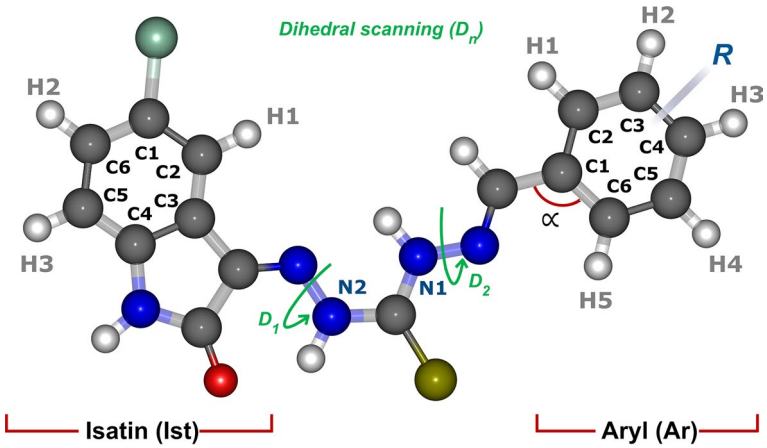

Fig. 1 Dihedral scanning of compounds **VI**–**X** by rotors D_1 and D_2; numbering of the atoms on the compounds (∝ is the angle between the aryl ring and imine group)

Bader's theory of atoms in molecules (AIM) [37, 38] was also used to determine the intramolecular interactions, ring critical points (RCPs) of the charge density distribution, and bond critical points (BCPs) of the bonding atoms. The electron density (ρ), potential energy density (V), intra-atomic dipole moment (μ_{intra}), and bond path length (BPL) of active phenolic hydrogen bonds were calculated and used for the analysis of antioxidant characteristics of the compounds. Furthermore, the ELF and NCI analyses were performed to determine electron localization and intramolecular interactions.

Results and discussion

Physical data

The physical data, yields, melting points, and elemental analysis results of the synthesized compounds are summarized in Tables 1 and 2, respectively.

Vibrational frequencies

In the FT-IR spectrum of the synthesized compounds, the aldehyde group (–CHO two bands) signal of the starting material was not observed near 2750–2650 cm^{-1}. Furthermore, the asymmetric and symmetric stretching bands of the amino group ($–NH_2$) were not shown at 3600–3200 cm^{-1}. These results were indicated a successful reaction as expected. In compounds **VI–X**, the –NH (isatin) stretching vibrations were observed at between 3185 and 3125 cm^{-1}. The C=O signals of isatin ring were observed at between 1702 and 1638 cm^{-1}, for compounds **VI–X**. In the compounds **VI–X**, the –C=N stretching vibrations were observed at 1621 and 1575 cm^{-1}. For those compounds, the C–Cl signals of isatin ring were observed at between 953 and 872 cm^{-1}. In compounds **VI–X**, the –C–O signals of phenyl ring were observed at between 1074 and 1059 cm^{-1} as shown in Fig. 2. For compounds **VI–X**, the –C=S stretching vibrations were shown at 1388 and 1328 cm^{-1}. The other remarkable absorption band, Ar-Br stretching vibration was appeared at around 674 cm^{-1} for compound **X**. These frequency values of the synthesized compounds are highly agreement with similar compounds [3, 4, 42]. Furthermore, both experimental and theoretical IR peaks of the compounds are given in Table 3. It is seen that the theoretical data were consistent with the experimental results. (All the IR spectra of the compounds are given in supplementary material A, Figs. S1–S4.)

^{1}H NMR spectra

The ^{1}H NMR spectra of the synthesized compounds were detected in DMSO-d_6 as the solvent. To evaluate the spectra, proton numbers of the compounds are shown in Fig. 1. In the compound **IX**, the aromatic proton signals of the aryl ring (H1, H4, and H5) were observed between 7.30 and 6.95 ppm (Fig. 3). The H1 proton

Table 1 Data for yields and melting points for the synthesized compounds

Comp.	Name	Color	Yield (%)	m.p. (°C)	Lit. yield (%)	Lit. m.p. (°C)
I	1-(2-hydroxybenzylidene)-thiocarbohydrazide	White	58	209	61	218 [39]
II	1-(2,4-dihydroxybenzylidene)-thiocarbohydrazide	Light yellow	52	215	58	214–215 [40]
III	1-(4-hydroxy-3-methoxybenzylidene)-thiocarbohydrazide	White	70	197	I	I
IV	1-(3-hydroxy-4-methoxybenzylidene)-thiocarbohydrazide	Light yellow	71	194	I	I
V	1-(5-bromo-2-hydroxybenzylidene) thiocarbohydrazide	White	82	> 300	85	302–304 [41]
VI	1-(2-hydroxybenzylidene)-5-(5-chloro-2-oxoindolin-3-ylidene) thiocarbohydrazone	Brown	68	256	N	N
VII	1-(2,4-dihydroxybenzylidene)-5-(5-chloro-2-oxoindolin-3-ylidene) thiocarbohydrazone	Light brownish Orange	65	261	N	N
VIII	1-(4-hydroxy-3-methoxybenzylidene)-5-(5-chloro-2-oxoindolin-3-ylidene) thiocarbohydrazone	Dark yellow	80	256	N	N
IX	1-(3-hydroxy-4-methoxybenzylidene)-5-(5-chloro-2-oxoindolin-3-ylidene) thiocarbohydrazone	Light orange	85	230	N	N
X	1-(5-bromo-2-hydroxybenzylidene)-5-(5-chloro-2-oxoindolin-3-ylidene) thiocarbohydrazone	Orange	63	282	N	N

Lit.: Literature, N: new compounds, I: They have CAS number but there is no the published article

Table 2 Results for elemental analysis for the synthesized compounds

Comp.	Calculated %			Experimental %		
	C	H	N	C	H	N
VI	51.358	3.236	18.724	51.049	3.183	18.783
VII	49.249	3.103	17.956	49.066	3.074	17.668
VIII	50.510	3.494	17.332	50.681	3.385	16.936
IX	50.510	3.494	17.332	49.970	3.437	17.217
X	42.408	2.449	15.461	42.240	2.418	15.389

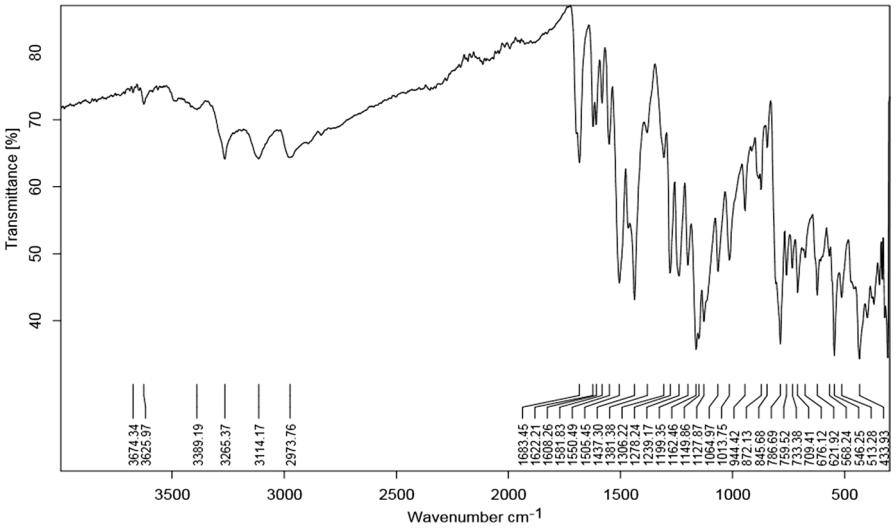

Fig. 2 Experimental FT-IR spectrum of compound **IX**

showed a singlet peak at 7.30–7.29 ppm. The H4 proton was coupled to the H5 proton and observed as doublet peaks at 7.24–7.22 ppm. The H5 proton was coupled to the H4 proton and detected as doublet peaks at 6.97–6.95 ppm. The signal of imin (–CH = N) was observed as a singlet peak at 8.04 ppm. The proton signals of thiocarbohydrazide regions occurred from $-N^1H$ and $-N^2H$. These amino peaks were observed as a singlet at 11.26 and 12.34 ppm, respectively. The hydroxyl group (–OH) proton signal was detected as a singlet at 8.95 ppm. The methoxy ($-OCH_3$) proton signal was detected as a singlet at 3.81 ppm. The amino (–NH) proton signal of isatin region was detected as a singlet in the range of 14.40 ppm. The aromatic proton signals of isatin ring (H1, H2, and H3) were observed between 7.49 and 6.91 ppm. The H1 proton was shown as a singlet peak at 7.49 ppm. The H2 proton was coupled to the H3 and H1 protons and observed as doublet of doublets peaks at 7.37–7.34 ppm. The H3 proton was coupled to the H2 proton and detected doublet peaks at 6.93–6.91 ppm. DMSO-d_6 and water in DMSO (HOD, H_2O) signals are shown around at 2.00, 2.50 (pentet), and 3.30 ppm (variable, depend on the solvent

Table 3 Experimental and calculated FT-IR values of the compounds (cm^{-1})

	Comp.	$\nu^{1}_{N\text{-}H}$	$\nu^{2}_{N\text{-}H}$	$\nu_{C\text{–}H\ (Ar.)}$	$\nu_{C=S}$	$\nu_{C=N}$	$\nu_{C\text{–}N}$	ν_{OH}	ν_{NH} (ist)	$\nu_{C\text{–}Cl}$	$\nu_{C=O}$ (ist)
Experimental	**VI**	3208	3195	3042	1370	1575	1195	3303	3129	950	1702
	VII	3314	3283	3023	1373	1582	1192	3223	3128	953	1687
	VIII	3383	3269	2987	1328	1582	1199	3127	3185	919	1697
	IX	3625	3389	2974	1381	1581	1199	3265	3114	872	1638
	X	3622	3394	3035	1388	1621	1198	3210	3125	882	1698
Calculated	**VI**	3646	3494	3204–3178	1362	1655	1197	3455	3431	1084	1752
	VII	3646	3495	3191–3171	1367	1656	1195	3829 *p*-OH 3416 *o*-OH	3432	1084	1750
	VIII	3647	3480	3222–3177	1364	1664	1191	3171	3435	1084	1750
	IX	3648	3479	3216–3190	1373	1644	1188	3787	3434	1084	1749
	X	3646	3494	32,017–3192	1356	1659	1199	3450	3430	1084	1752

ist: Isatin

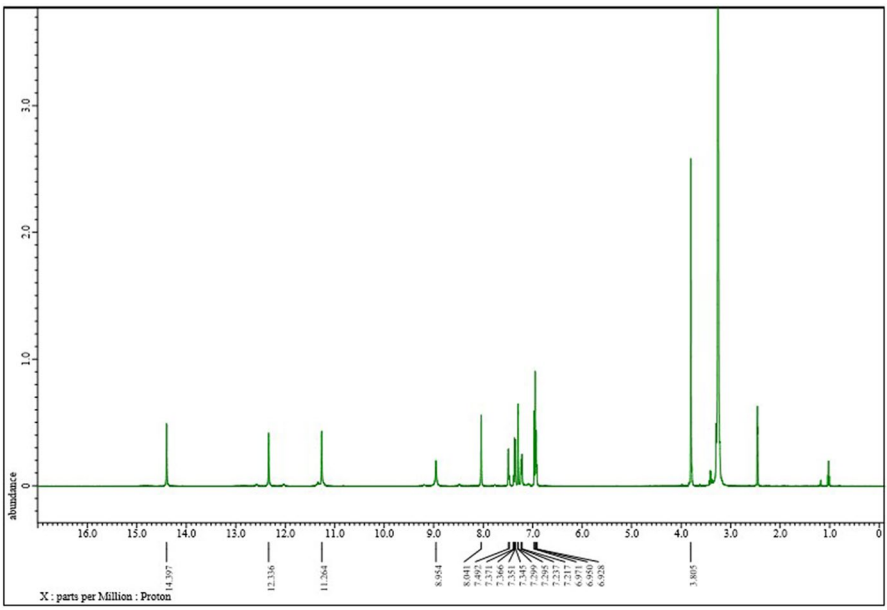

Fig. 3 Experimental ^{1}H NMR spectrum of compound **IX**

and its concentration), respectively [43]. These data are conformable with the values of those reported previously for similar compounds [3, 4, 42]. Both experimental and theoretical proton chemical shift values of the synthesized compounds are given in Table 4. (All the ^{1}H NMR spectra of the other compounds are given in supplementary material A, Figs. S5–S8.)

^{13}C NMR spectra

The ^{13}C NMR spectra of all compounds were obtained in DMSO-d_6. To evaluate the spectra, each carbon atom number of the compounds is shown in Fig. 1. The ^{13}C NMR spectrum of the compound **IX** showed 17 different resonances in good agreement with the proposed structure in Fig. 4. In compound **IX**, methyl-substituted aromatic carbon (–OCH_3) was observed at 56.1 ppm, and –C=S signal of thiocarbohydrazide region was detected at 175.6 ppm. The characteristic –CH=N (imin) peak was observed at 147.4 ppm. The carbonyl atom (–C=O) of isatin region was observed at 163.0 ppm. The –C=N atom of isatin ring were appeared at 131.1 ppm. The aromatic carbons (C1–C6) of the aryl region were also observed at 127.0, 126.8, 145.8, 150.9, 113.0, and 112.6 ppm, respectively. The resonances of the C3 and C4 carbon atoms shifted downfield due to the presence of –OH and –OCH_3 groups, respectively. The aromatic carbons (C1–C6) of isatin region were also observed at 137.1, 121.1, 122.5, 141.5, 114.5, and 132.0 ppm, respectively. The resonances of the C1 and C4 carbon atoms shifted downfield due to the presence of –Cl and –NH

Table 4 ^{1}H NMR (δ, ppm, in DMSO-d_6) values related to the synthesized compounds

	Comp.	–CH=N	–N^2H–N	=N–N^1H	–Ar H	–OH	–OCH_3	Isatin ArH	Isatin NH
Experimental	**VI**	8.5	12.4	11.3	8.0–8.0 (1H) 7.3–7.2 (1H) 6.9–6. 9 (1H) 6.8–6.8 (1H)	10.0	–	7.7 (1H) 7.5–7.4 (1H) 7.4-7.3 (1H)	14.4
	VII	8.7	12.3	11.2	7.8–7.8 (1H) 6.3–6.3 (1H) 6.9–6. 9 (1H)	9.9 *o*-OH 8.4 *p*-OH	–	7.7 (1H) 7.5–7.4 (1H) 7.4-7.3 (1H)	14.3
	VIII	8.0	12.3	11.3	7.3–7.3 (1H) 7.2–7.2 (1H) 7.0–6.9 (1H)	9.0	3.80	7.5 (1H) 7.4 (1H) 6.9 (1H)	14.4
	IX	8.0	12.3	11.3	7.3–7.3 (1H) 7.2–7.2 (1H) 7.0–6.9 (1H)	9.0	3.81	7.5 (1H) 7.4–7.3 (1H) 6.93–6.91 (1H)	14.4
	X	8.4	12.5	11.3	8.1 (1H) 7.0–6.8 (2H)	10.4	–	7.5 (1H) 7.4 (2H)	14.4

Table 4 (continued)

	Comp.	–CH=N	$-N^2H-N$	$=N-N^1H$	–Ar H	–OH	$-OCH_3$	Isatin ArH	Isatin NH
Calculated	**VI**	8.9	13.3	11.1	7.9 (H3) 7.8 (H1) 7.5 (H2) 7.5 (H4)	11.7	–	8.0 (H1) 7.8 (H2) 7.3 (H3)	7.6
	VII	8.8	13.2	10.9	7.7 (H1) 6.9 (H2) 6.7 (H4)	11.9 *o*-OH 5.3 *p*-OH	–	8.0 (H1) 7.8 (H2) 7.3 (H3)	7.5
	VIII	8.6	13.2	11.1	8.1 (H5) 7.4 (H2) 7.3 (H1)	6.4	4.5–4.1	8.0 (H1) 7.8 (H2) 7.3 (H3)	7.5
	IX	8.6	13.2	11.0	8.3 (H5) 7.4 (H1) 7.4 (H4)	5.8	4.5–4.0	8.1 (H1) 7.7 (H2) 7.3 (H3)	7.5
	X	8.8	13.3	11.1	7.9 (H3) 7.8 (H1) 7.4 (H4)	11.7	–	8.0 (H1) 7.8 (H2) 7.3 (H3)	7.5

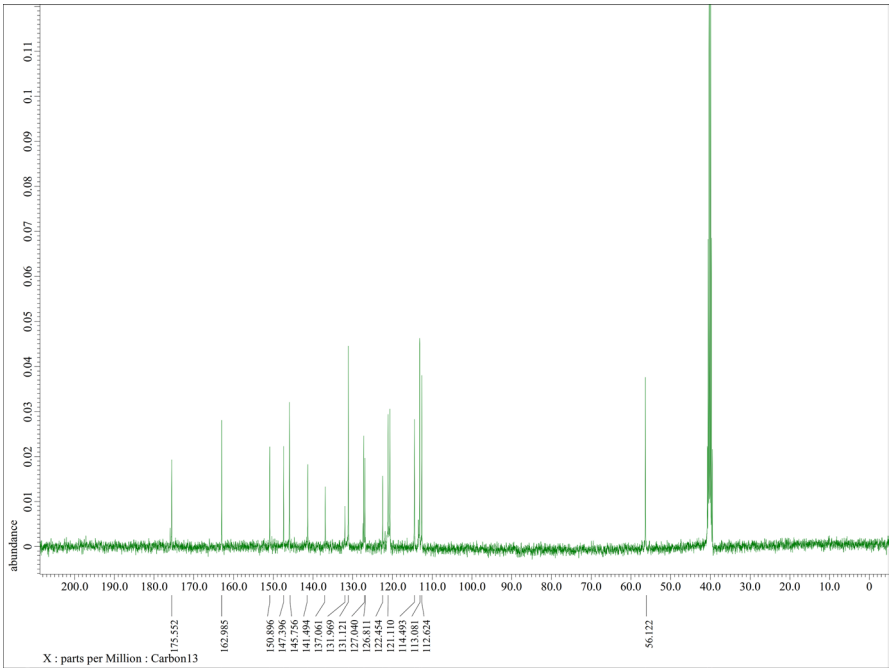

Fig. 4 Experimental ^{13}C NMR spectrum of compound **IX**

groups, respectively. These spectroscopic data are consistent with the values of reported formerly similar compounds in the literature [3, 4, 42]. Both experimental and theoretical proton chemical shift values of the compounds are given in Table 5. (All the ^{13}C NMR spectra of the other compounds are given in supplementary material A, Figs. S9–S12.)

Antioxidant activity assays

It was used trolox as a standard to compare antioxidant activities of the compounds. The percentage inhibition changes due to the concentration of the trolox and synthesized compounds are given in Fig. 5.

Compounds **VII** and **VIII** showed an increased free radical scavenging activity depending on concentration. On the other hand, compounds **VI**, **IX**, and **X** exhibited a regular percent inhibition increase after 0.5 µM concentration. These inhibition increases vary with the excess and location of the phenolic structures. Accordingly, compounds **VII** and **VIII** showed the greatest increase in inhibition. Similar to our study, Naik et al. reported that although isatin exhibited negligible antioxidant activity, the binding of substituted anilines is significantly increased efficacy. In particular, among the compounds they synthesized, compounds containing an

Table 5 ^{13}C NMR (δ, ppm, in DMSO-d_6) values related to synthesized compounds

	Comp.	C=S	–CH=N	Ar C1	Ar C2	Ar C3	Ar C4	Ar C5	Ar C6	CH_3	C=N	C=O	ist C1	ist C2	ist C3	ist C4	ist C5	ist C6
Exp.	**VI**	175.4	152.0	120.0	132.8	126.6	142.2	113.2	157.8	–	140.9	163.0	131.1	120.7	122.2	136.9	116.8	127.5
	VII	175.9	146.3	120.5	131.9	113.1	174.9	112.3	152.5	–	129.6	162.9	136.4	122.5	127.2	141.2	121.1	130.9
	VIII	175.8	147.5	126.9	122.5	114.5	150.7	146.0	112.6	56.4	127.2	163.0	137.0	120.6	121.1	141.3	113.2	131.1
	IX	175.6	147.4	127.0	126.8	145.8	150.9	113.0	112.6	56.1	131.1	163.0	137.1	121.1	122.5	141.5	114.5	132.0
	X	175.8	140.4	119.1	132.0	127.3	134.9	113.5	156.9	–	128.6	162.9	137.3	120.6	121.9	141.4	111.5	131.2
Calculated	**VI**	180.4	157.5	122.6	137.8	123.3	137.9	120.3	166.9	–	134.6	167.3	140.9	125.3	126.9	146.7	116.0	136.4
	VII	179.6	156.9	115.5	139.8	110.1	167.6	104.6	168.6	–	134.3	167.3	140.9	125.1	127.0	146.5	116.0	136.2
	VIII	180.5	156.2	130.4	131.3	116.6	157.6	152.7	108.2	56.3	133.9	167.2	140.7	125.0	127.1	146.4	115.9	136.0
	IX	180.6	155.9	130.9	121.2	151.6	155.7	114.5	120.4	56.3	135.0	167.1	140.3	125.6	127.3	146.2	116.0	136.0
	X	180.7	155.9	124.2	139.2	133.3	140.2	122.4	165.7	–	134.9	167.3	141.0	125.4	126.8	146.8	116.0	136.5

ist: Isatin

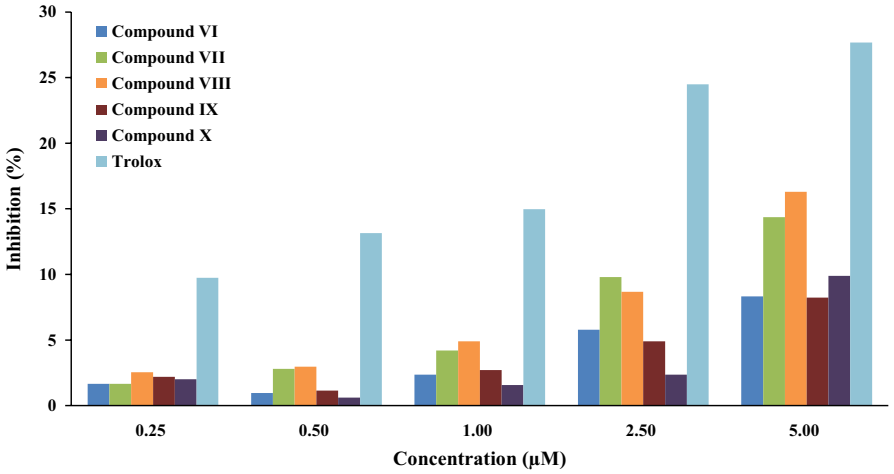

Fig. 5 Inhibition (%) calculated by the DPPH method for compounds **VI–X** and trolox at different concentrations

electron-donating methoxy substituent, they have had higher antioxidant activity compared to butylated hydroxyanisole (BHA) [44].

In order to compare the free radical scavenging effects of the trolox and the synthesized compounds, concentration equations were obtained and are shown in Table 6 together with IC_{50} values. According to IC_{50} values, antioxidant activities of synthesized compounds were found to be trolox > **VIII** > **VII** > **X** > **VI** > **IX**.

The electronic effects of substituent groups on thiocarbohydrazone play an important role in antioxidant activity [45]. Previously, it has been reported that halogen-containing systems effectively increase antioxidant potency [17, 46].

Similarly, in our study, the halogen-containing molecule (compound **X**) on aldehyde showed more antioxidant effects than the halogen-free molecule (compound **VI**). However, this is quite low compared to methoxy-containing molecules. In particular, as shown in compound **VIII**, the methoxy groups exhibited the highest antioxidant effect when attached to the structure at the *meta* position.

Table 6 Concentration equation and IC_{50} values of compounds **VI–X** by DPPH method

Compounds	Concentration Eq. (0.25–5.0) × 10^{-6} M	R^2	IC_{50} (µM)
Trolox	$y = 3.688x + 11.181$	0.890	10.525
VI	$y = 1.553x + 0.945$	0.940	31.593
VII	$y = 2.692x + 1.587$	0.964	17.983
VIII	$y = 2.893x + 1.724$	0.998	16.690
IX	$y = 1.409x + 1.229$	0.957	34.614
X	$y = 1.768x + 0.022$	0.812	28.268

Andreani et al. examined the interaction of phenolic and $–CH_3$ groups in the *ortho* position relative to each other in the benzene ring and found that the $–CH_3$ group reduced antioxidant activity. In another molecule synthesized in the same study, it was found that –OMe group bound structures known to have weak free radical scavenging power exhibit surprisingly good antioxidant activity [47]. Similarly, in this study, the effectiveness of –OMe groups bound to benzene rings for compound **VIII** can be mentioned. However, as in example compounds **VIII** and **IX**, it is one of the important conclusions drawn in this study that the location of the –OMe groups significantly affected the antioxidant activity.

Theoretical analysis

In phenolic compounds that are widely studied and useful as antioxidants, the chemical structure and position of –OH groups affect the antioxidant activity of the compounds. Structures containing methoxy groups also play an important role in determining antioxidant characteristics of a compound. In this context, the compounds were structurally analyzed in two groups: The first group was compounds **VI**, **VII,** and **X** containing *ortho* OH, in which the effects of *p*-OH and *m*-Br substituents on antioxidant characteristics were investigated. The second group consisted of compounds **VIII** and **IX**, and their antioxidant characteristics were analyzed according to the sequential change of the positions of phenolic –OH and methoxy substituents.

Prereaction and postreaction energies of the compounds with DPPH• and differences between these energies (Δ_E), FMO energies, HOMO–LUMO energy gap (ΔE_g), electronegativity (χ) values, and chemical hardness (η) values are given in Table 7. The stability of a molecule is directly dependent on the energy gap (ΔE_g), difference between HOMO and LUMO energies. In the first group, the ΔE_g values of the compounds were the smallest for compound **VII** (2.859 eV) and the largest for compound **VI** (2.980 eV). Similarly, for the compounds in the second group, ΔE_g of the compound **VIII** (2.828 eV) was lower than that of the compound **IX** (2.855 eV). Compounds having a lower ΔE_g value were found to have a higher tendency to react with DPPH$^{\bullet}$, i.e., a direct proportion between the antioxidant properties of the compounds and ΔE_g was observed. Besides, concentrating on the active phenolic hydrogen bonds and electronic properties of these bonds, which play a key role in the reaction of the compounds with DPPH$^{\bullet}$, is more useful for analyzing the reaction mechanism.

Systems are easier to react that require low threshold energy or require lower energy. The Δ_E values between the energies of the compounds in the neutral and oxidized state were calculated to be approximately 416.93, 405.75, 415.93 kcal/mol for the first group and 403.02, 404.52 kcal/mol for the second group, respectively (Table 7). The calculations showed that the compounds with higher antioxidant properties had lower Δ_E. In other words, consistent with the experimental results, the compounds that required more energy for reaction with DPPH$^{\bullet}$ had weaker antioxidant activity. Moreover, a similar relationship was observed for the chemical hardness of the compounds. Chemical hardness has an important effect

Table 7 Calculated electronic and geometrical parameters of the compounds

Comp.	E (kcal/mol)	E (kcal/mol) (oxidized)	Δ_E (kcal/mol)	E_{HOMO} (eV)	E_{LUMO} (eV)	ΔE_g (eV)	χ (eV)	η	$\propto$ (°)
VI	− 1192189.032	− 1191772.099	416.9331	− 6.177	− 3.197	2.980	4.687	1.490	122.209
VII	− 1,239,410.691	− 1,239,004.937	405.7545	− 6.005	− 3.146	2.859	4.575	1.430	122.193
VIII	− 1,264,072.893	− 1,263,669.875	403.0181	− 5.867	− 3.0389	2.828	4.453	1.414	121.033
IX	− 1,264,071.300	− 1,263,666.777	404.5227	− 5.859	− 3.004	2.855	4.431	1.428	122.098
X	− 2,807,108.370	− 2,806,692.436	415.9345	− 6.254	− 3.286	2.968	4.770	1.484	122.295
DPPH•	− 890,000.97		397.51	− 5.97	− 3.31	2.66	4.64		
DPPH	− 890,398.49			− 6.40	− 3.67	2.73	5.04		

DPPH•: Radical DPPH, DPPH: reduced DPPH, E: Energy, $\Delta_E = E_{oxidized} - E$, ΔE: $E_{LUMO} - E_{HOMO}$, χ: electronegativity, η: chemical hardness, $\propto$: angle between the phenyl ring and imine group

on determining (or controlling) chemical reactivity of compounds. Accordingly, the compounds with lower chemical hardness were observed to exhibit higher antioxidant properties.

HOMO-ESP maps of the compounds are given in Fig. 6 (isovalue of MOs was taken as 0.003 for better examination of HOMO).

In the first group compounds, the HOMO distribution of *o*-OH substituent showed an overlapping spread with that of the sulfur atom, which is due to the intramolecular interaction of the phenolic *o*-OH and sulfur-imine group. (This situation will be further investigated in AIM analysis.) The probability of exposure to steric effect due to the location of the *p*-OH substituent was lower than the

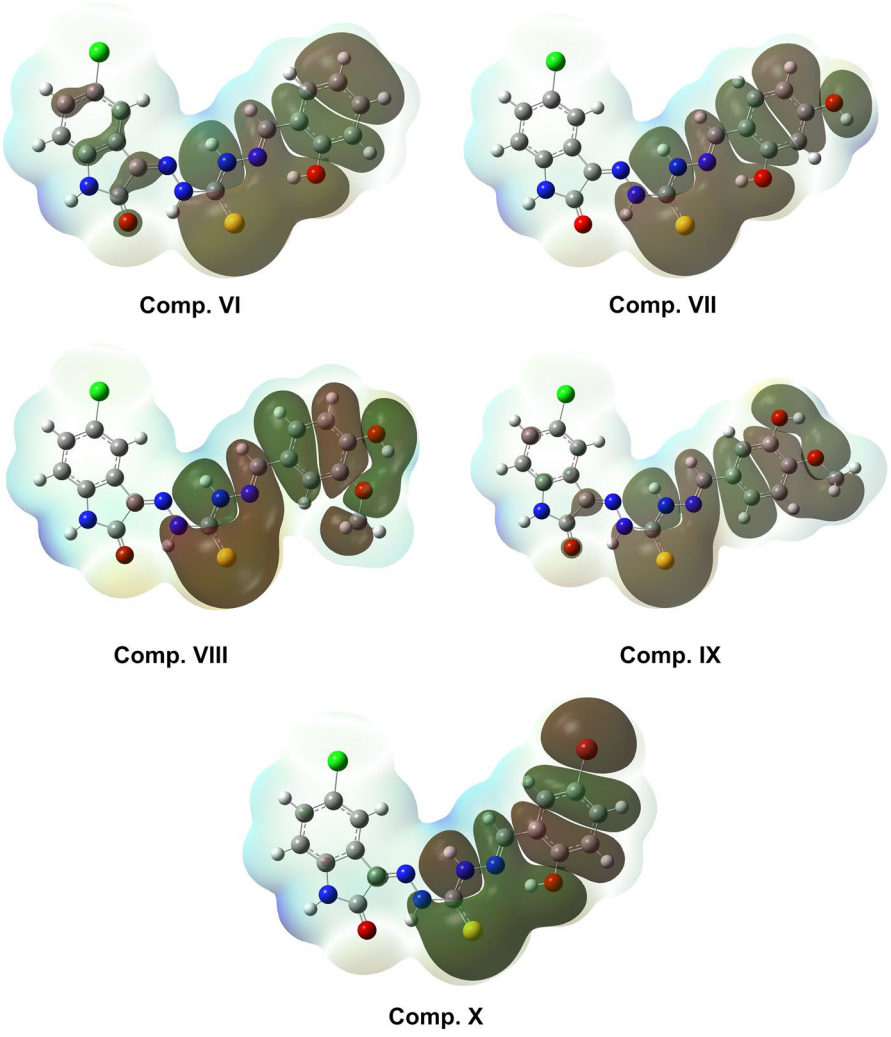

Fig. 6 HOMO with ESP maps of compounds

others as well as its electron donor behavior made compound **VII** more reactive to DPPH•, in the first group. Besides, the electronegative effect of the bromine atom on the electron distribution of the O–H bond in compound **X** caused it to exhibit more antioxidant property than compound **VI**.

In the second group of compounds, the *o*- and *p*- positions of the –OH and methoxy substituents had a major effect on the reactivity of the compounds. Phenolic –OH substituent is more electronegative than methoxy. In both compounds, the *para*-substituents give electrons to the benzene ring with resonance effect, whereas *meta* substituents exhibit inductively electron-withdrawing behavior. In the *p*-OH substituted compound **VIII**, both the electronegativity and the positional effect of the substituted group caused the O–H bond to be weaker and therefore caused it to be more reactive to DPPH• than compound **IX**.

Concentrating on the active phenolic hydrogen bonds and electronic properties of these bonds will provide much more detailed information in the analysis of the antioxidant properties of the compounds. For this purpose, AIM, NCI, and ELF analysis were performed. AIM analysis was performed to determine intramolecular interactions and their electronic properties, the RCPs of the charge density distribution, and the BCPs of the bonding atoms. The AIM calculations revealed a significant correlation between the antioxidant properties of the compounds and the electron charge density (ρ), delocalization index (DI), potential energy density (V), ellipticity, bond length (L), and bond path length (BPL) of the phenolic hydrogen bonds on the substitute groups.

AIM and NIC visualization of compound **VI** is given Fig. 7. (AIM and NIC visualizations of the compounds are given supplementary material B.) There is a very strong interaction between *o*-OH and imine group compared to other intramolecular interactions.

The antioxidant property of a compound is proportional to the amount of DPPH that reacts with the compound. The reaction DPPH• + RH→DPPH + R• shows that a compound with weak active hydrogen bonds exhibits a higher antioxidant characteristic. In the application of this method, the proton transfer reaction to DPPH free radical by the antioxidant causes a decrease in absorbance at 517 nm. Antioxidants can be classified as primary antioxidants (chain breaker) and secondary antioxidants

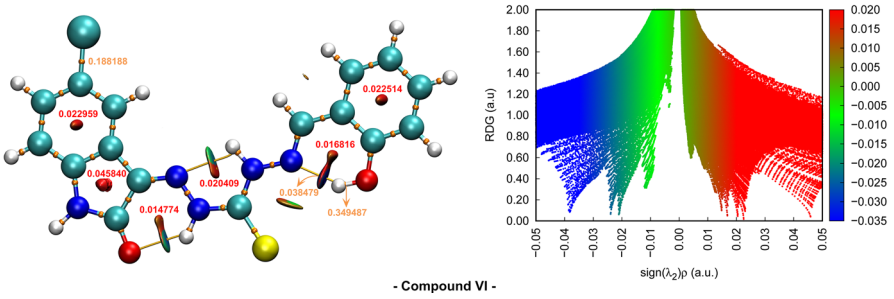

Fig. 7 AIM and NIC visualizations of compound **VI**; Brown points: bond critical points, Red points: ring critical points, Dashed lines: interactions of respective atoms

(preventive) according to their mechanism of action. Primary antioxidants break the oxidation chain reaction by giving hydrogen and generate more stable radicals. Secondary antioxidants slow the oxidation reaction rate by many mechanisms such as chelating metals, regenerating primary antioxidants, degrading hydroperoxides, and absorbing oxygen and other species [48, 49]. According to these classifications, some antioxidants may show more than one mechanism of action. In this article, the antioxidant mechanisms of the synthesized compounds (**VI–X**) are tried to be elucidated based on the primary antioxidant mechanisms. Phenolic structures in synthesized compounds are generally considered as proton provider basic groups to explain the antioxidant mechanism.

Although the active hydrogen bonds in the reaction are influenced by factors such as intramolecular interactions and temperature, the bond strength is proportional to the electron density (ρ) of the bond. It can be said that as the charge density of the O–H bond decreases, the bond strength decreases and it is easier to break off the hydrogen from the compounds, and hence, these compounds exhibit high antioxidant properties [50, 51]. The data obtained by the AIM analysis are given in Table 8.

The *o*- and *p*-hydroxyl group exhibits an electron donor behavior by resonance effect on the phenyl ring in conjugation with the benzene π system. The strong intramolecular interaction between the imine group and *o*-OH allowed electron delocalization. In compound **VII**, the electron donor effect of *p*-OH caused an increase in BCP charge density between imine group and *o*-OH (0.038479 au for compound **VI** and 0.039714 au for compound **VII**). Besides, this interaction caused the angle between the imine group and the phenyl ring to decrease (α is 122.209 degree for compound **VI**, 122.193 degree for compound **VII**). In the two groups, it was observed that the angle ∝ varied according to the degree of intramolecular interactions (∝ values are given in Table 7). As a result of strong intramolecular interaction and electron delocalization, the electron density of the *o*-(O–H) bond of compound **VII** (0.346878 au) decreased compared to compound **VI** (0.349482 au), which caused the bond to weaken (Table 8). This weaker O–H bond facilitated the reaction of the compound with DPPH•, thereby contributing to its antioxidant properties. Also, the presence of both *o*- and *p*-OH in compound **VII** increased its reaction possibility with the DPPH• compared to compound **VI**. In Compound **X**, the *m*-Br

Table 8 AIM data of phenolic hydrogen bonds

Comp.	ρ (au)	DI	μ_{intra}	V (au)	K (au)	Ellipticity	BPL (Å)	L (Å)
VI	0.349482	0.500370	0.2191	− 0.800384	0.730924	0.015244	1.802381	0.98039
VII	0.374222	0.656726	0.1625	− 0.838785	0.763841	0.019844	1.769760	0.96226
	0.346878*	0.493734*	0.1219*	− 0.794387*	0.725253*	0.015044*	1.806483*	0.98250*
VIII	0.368970	0.604483	0.1466	− 0.833768	0.761776	0.019032	1.775860	0.96610
IX	0.370073	0.611293	0.1484	− 0.835761	0.762916	0.019965	1.774148	0.96513
X	0.348897	0.498284	0.1234	− 0.799238	0.730067	0.015141	1.802984	0.98074

*Values for *o*-(O–H) bond, ρ: electron charge density, DI: delocalization index, μ_{intra}: magnitude of Intra-atomic dipole moment of phenolic H, V: potential energy density, K: kinetic energy density, L: bond length, *BPL*: bond path length

substituent exerted electron-withdrawing inductive effect, resulting in a decrease in the BCP electron density of the *o*-(O–H) bond (0.348897 au). The AIM data of the first group of compounds revealed that there was an inverse relationship between the BCP electron density of the *o*-(O–H) bond and the antioxidant property.

It was seen in theoretical calculations that the methoxyl group forms intramolecular hydrogen bonding with phenolic hydrogen and facilitates phenolic H-atom abstraction. There are also studies that the methoxyl group increases the antioxidant activity of the related compound as a result of intramolecular interaction with phenolic *p*-OH [52–55]. Besides, the position of phenolic –OH and methoxy groups is also one of the important variables affecting the antioxidant properties [56]. The *o*-OH substituent of compound **VII** exhibits electron donor behavior with resonance effect, while the *m*-OCH_3 substituent of compound **VIII** inductively exhibits electron-withdrawing behavior. Although the inductive effect is weaker than the resonance effect, in compound **VII** both –OH substituents pump electrons into the ring as an electron donor, while the *m*-methoxy substituent of compound **VIII** exhibits an electron-withdrawing effect. Although more electron delocalization is expected on *p*-OH in compound **VIII** due to the opposite behavior of the substituted groups, electron delocalization in compound **VIII** is lower due to the overlapping of the molecular orbitals of *m*-OCH_3 and *p*-OH. Electron localization is an important tool in understanding the behavior of compounds (see Fig. 8, all the ELF isosurfaces of the compounds are given supplementary material B), and the delocalization index is influenced by both bond-forming atoms and the environment. The increase in the number of localized electrons naturally causes a decrease in the number of delocalized electrons, and thus, the resulting polarity reduces the DI. When the groups examined, it was observed that the compounds having lower DI values showed high antioxidant properties.

The BCP charge density of the *p*-(O–H) bond (0.368970 au) of compound **VIII** was lower than that of the compound **IX** compared to the *m*-(O–H) bond (0.370073 au), which caused it to exhibit higher antioxidant properties compared to compound **IX**.

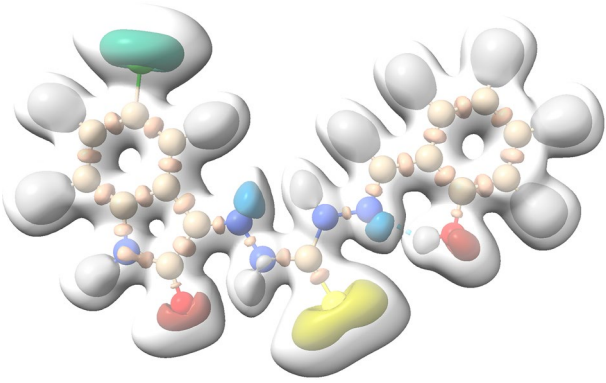

Fig. 8 ELF isosurface of compound **VI**

Furthermore, *o*-(O–H) bond length (L) and BPL are inversely proportional to potential energy, and compounds with larger bond length exhibit higher antioxidant properties, resulting in a correlation between the potential energy density of O–H bond and the antioxidant property of the compound. The calculations showed that the similar correlations between the electronic data of the relevant groups and the antioxidant properties were also valid for V, K, μ_{intra}, and ellipticity values (Table 8).

Conclusion

Substituted isatin-thiocarbohydrazones based on Schiff bases are commonly called as β-isatin aldehyde-*N*,*N*′-thiocarbohydrazones. They were synthesized with yields of 63–85%. All the products were characterized by FT-IR, ^{1}H NMR, and ^{13}C NMR spectroscopic techniques and elemental analyses. The in vitro antioxidant properties of the compounds were measured by DPPH free radical scavenging method. Among the synthesized compounds, the highest antioxidant activity showed the compound **VIII**, which exhibits an IC_{50} value close to the trolox used as the standard antioxidant. It was observed that the positions of methoxy and hydroxyl groups relative to each other were effective on antioxidant activity. It was concluded that the methoxy group forms an intramolecular hydrogen bond with phenolic OH, thus facilitating H-atom abstraction by reducing the bond dissociation enthalpy of the phenolic hydroxyl group. DFT/B3LYP/6-311++g(2d,2p) method was used for the quantum chemical calculations. BPL and *L*, which depend on the electron charge density and potential density on the phenolic O–H bonds, were also parameters that are easily calculated for determining the degree of antioxidant activity of the compounds. It was shown that there was a correlation between the inter-atomic dipole moments and ellipticity of the phenolic hydrogens and the antioxidant properties of the compounds. The interaction of the phenolic O–H bond with the surrounding atom groups determines DI, and calculations revealed that the compounds with smaller electron delocalization index showed higher antioxidant properties.

Authors contribution HY was involved in synthesis, structure elucidation, and writing-original draft preparation. HM was involved in synthesis, methodology, and structure elucidation. TKB was involved in antioxidant activity studies and writing-original draft preparation. MSÇ was involved in density functional theory calculations and writing-original draft preparation.

Compliance with ethical standards

Conflict of interest The authors declare that they have no conflict of interest.

References

1. S.N. Pandeya, S. Smitha, M. Jyoti, S.K. Sridhar, Acta Pharm. **55**, 27 (2005)
2. Z.H. Chohan, H. Pervez, A. Rauf, K.M. Khan, C.T. Supuran, J. Enzyme Inhib. Med. Chem. **19**, 417 (2004)

3. S.Y. Abbas, A.A. Farag, Y.A. Ammar, A.A. Atrees, A.F. Mohamed, A.A. El-Henawy, Monat. Chem. **144**, 1725 (2013)
4. A. Jarrahpour, D. Khalili, E. De Clercq, C. Salmi, J. Brunel, Molecules **12**, 1720 (2007)
5. A.V. Bogdanov, I.F. Zaripova, A.D. Voloshina, A.S. Strobykina, N.V. Kulik, S.V. Bukharov, J.K. Voronina, A.R. Khamatgalimov, V.F. Mironov, Monat. Chem. **149**, 111 (2018)
6. H. Muğlu, Res. Chem. Intermed. **46**, 2083 (2020)
7. T.K. Bakır, J.B. Lawag, Res. Chem. Intermed. **46**, 2541 (2020)
8. M. Verma, S.N. Pandeya, K.N. Singh, J.P. Stables, Acta Pharm. **54**, 49 (2004)
9. T. Aboul-Fadl, F.A. Bin-Jubair, Int. J. Res. Pharm. Sci. **1**, 113 (2010)
10. T.R. Bal, B. Anand, P. Yogeeswari, D. Sriram, Bioorg. Med. Chem. Lett. **15**, 4451 (2005)
11. D. Sinha, A.K. Tiwari, S. Singh, G. Shukla, P. Mishra, H. Chandra, A.K. Mishra, Eur. J. Med. Chem. **43**, 160 (2008)
12. S. Pandeya, D. Sriram, Acta Pharm. Turcica **40**, 33 (1998)
13. D. Sriram, S. Pandeya, G. Nath, E. De Clercq, Arzneimittelforschung **50**, 55 (2000)
14. M. Sathisha, V. Revankar, K. Pai, Met. Based Drugs **2008** (2008)
15. C. Liang, J. Xia, D. Lei, X. Li, Q. Yao, J. Gao, Eur. J. Med. Chem. **74**, 742 (2014)
16. M.T. Gabr, N.S. El-Gohary, E.R. El-Bendary, M.M. El-Kerdawy, N. Ni, Eur. J. Med. Chem. **128**, 36 (2017)
17. G. Kiran, M. Sarangapani, T. Gouthami, A.R. Narsimha Reddy, Toxicol. Environ. Chem. **95**, 367 (2013)
18. K. Gangarapu, S. Manda, A. Jallapally, S. Thota, S.S. Karki, J. Balzarini, E. De Clercq, H. Tokuda, Med. Chem. Res. **23**, 1046 (2014)
19. P. Wanasundara, F. Shahidi, *Antioxidants: Science, Technology, and Applications*, 6th edn. (Wiley Interscience, Hoboken, 2005)
20. G. Kiran, T. Maneshwar, Y. Rajeshwar, M. Sarangapani, J. Chem. **2013** (2013)
21. M. Premanathan, S. Radhakrishnan, K. Kulangiappar, G. Singaravelu, V. Thirumalaiarasu, T. Sivakumar, K. Kathiresan, Indian J. Med. Res. **136**, 822 (2012)
22. A.I. Elshamy, T. Yoneyama, N. Van Trang, N.T. Son, Y. Okamoto, S. Ban, M. Noji, A. Umeyama, J. Mol. Struct. **1200**, 127061 (2020)
23. N.T. Son, D.T.M. Thanh, N. Van Trang, J. Mol. Struct. **1193**, 76 (2019)
24. T.S. Ahamed, V.K. Rajan, K. Sabira, K. Muraleedharan, Comput. Biol. Chem. **80**, 66 (2019)
25. S. Yu, Y. Wang, Y. Ma, L. Wang, J. Zhu, S. Liu, Inorg. Chim. Acta **468**, 159 (2017)
26. W. Brand-Williams, M.-E. Cuvelier, C. Berset, LWT-Food Sci. Technol. **28**, 25 (1995)
27. D. Huang, B. Ou, R.L. Prior, J. Agric. Food Chem. **53**, 1841 (2005)
28. S. Mukherjee, N. Pawar, O. Kulkarni, B. Nagarkar, S. Thopte, A. Bhujbal, P. Pawar, BMC Complement. Altern. Med. **11**, 38 (2011)
29. W. Kohn, L.J. Sham, Phys. Rev. **140**, A1133 (1965)
30. P. Hohenberg, W. Kohn, Phys. Rev. **136**, B864 (1964)
31. M. Frisch, G. Trucks, H. Schlegel, G. Scuseria, M. Robb, J. Cheeseman, G. Scalmani, V. Barone, B. Mennucci, G. Petersson, D. Fox, Wallingford (2010)
32. R. Bader, *Atoms in Molecule* (Oxford University Press, Oxford, 1990)
33. A.E. Reed, L.A. Curtiss, F. Weinhold, Chem. Rev. **88**, 899 (1988)
34. J. Carpenter, F. Weinhold, J. Mol. Struct: Theochem **169**, 41 (1988)
35. A.E. Reed, F. Weinhold, J. Chem. Phys. **78**, 4066 (1983)
36. A.E. Reed, R.B. Weinstock, F. Weinhold, J. Chem. Phys. **83**, 735 (1985)
37. R.F. Bader, Chem. Rev. **91**, 893 (1991)
38. R.F. Bader, Acc. Chem. Res. **18**, 9 (1985)
39. V.V. Dabholkar, D.R. Tripathi, Indian J. Chem. Sec. B **49B**, 593 (2010)
40. Z. Shi, Z. Zhao, M. Liu, X. Wang, Comptes Rendus Chim. **16**, 977 (2013)
41. A. Abdel-Aziem, B.S. Baaiu, A.O. Abdelhamid, J. Heterocycl. Chem. **54**, 3471 (2017)
42. O. Bekircan, H. Bektas, Molecules **13**, 2126 (2008)
43. I. Fleming, D.H. Williams, *Spectroscopic Methods in Organic Chemistry* (McGraw-Hill, New York, 1966)
44. N. Naik, H. Vijay Kumar, P.B. Vidyashree, J. Pharm. Res. **4**, 2686 (2011)
45. A. Božić, N. Filipović, I. Novakovic, S. Bjelogrlić, J. Nikolić, S. Drmanić, A. Marinković, J. Serb. Chem. Soc. **82**, 495 (2017)
46. G. Sammaiah, G. Brahmeshwari, M. Sarangapani, J. Adv. Pharm. Sci. **1**, 47 (2011)

47. A. Andreani, S. Burnelli, M. Granaiola, A. Leoni, A. Locatelli, R. Morigi, M. Rambaldi, L. Varoli, M.A. Cremonini, G. Placucci, Eur. J. Med. Chem. E **45**, 1374 (2010)
48. F. Shahidi, H.J. Zhong, P. Ambigaipalan, Bailey's industrial oil and fat products **6**, 491 (2005)
49. F. Shahidi, Y. Zhong, J. Agric. Food Chem. **59**, 8 (2011)
50. M.S. Çavuş, H. Yakan, H. Muğlu, T. Bakır, J. Phys. Chem. Solids **140**, 109362 (2020)
51. H. Muğlu, M.S. Çavuş, T. Bakır, H. Yakan, J. Mol. Struct. **1196**, 819 (2019)
52. J. Chen, J. Yang, L. Ma, J. Li, N. Shahzad, C.K. Kim, Sci. Rep. **10**(1), 2611 (2020)
53. J.-C. Cheng, F. Dai, B. Zhou, L. Yang, Z.-L. Liu, Food Chem. **104**, 132–139 (2007)
54. M.I. de Heer, P. Mulder, H.-G. Korth, K.U. Ingold, J. Lusztyk, J. Am. Chem. Soc. **122**, 2355–2360 (2000)
55. R. Farhoosh, S. Johnny, M. Asnaashari, N. Molaahmadibahraseman, A. Sharif, Food Chem. **194**, 128 (2016)
56. J.S. Wright, E.R. Johnson, G.A. DiLabio, J. Am. Chem. Soc. **123**, 1173 (2001)